A MECHANICAL ANALYSIS OF MYOMERE SHAPE IN FISH

JOHAN L. VAN LEEUWEN*

Experimental Zoology Group, Wageningen Institute of Animal Sciences (WIAS), Wageningen University, Marijkeweg 40, NL-6709 PG Wageningen, The Netherlands

*e-mail: johan.vanleeuwen@morf.edc.wag-ur.nl

Summary

An architectural analysis is offered of the trunk muscles in fish, which are arranged in a longitudinal series of geometrically complex myomeres. The myomeres are separated by myosepta, collagenous sheets with complex fibre patterns. The muscle fibres in the myomeres are also arranged in complex three-dimensional patterns. Previously, it has been proposed that the muscle fibre arrangement allows for a uniform strain distribution within the muscle. Physical constraints limit the range of shapes that fibre-reinforced materials such as muscles can adopt, irrespective of their genetic profile. The three-dimensional shapes of myosepta are predicted by mechanical modelling from the requirements for mechanical stability and prescribed muscle fibre arrangements. The model can also be used to study the force transmission and likely locations of ligaments and bones in the myosepta. The model shows that the dorsal and ventral fins are located such that unfavourable mechanical interactions with the trunk muscles are avoided. In bony fish, extensive muscular deformations (notably in the region of the horizontal septum) that would not contribute to bending are avoided by the mechanical support of the skin, intramuscular bones and ribs. In sharks, the skin plays a more prominent role in avoiding such deformations because of the absence of bony elements.

Key words: biomechanical model, collagen fibre, elasmobranch, fish, locomotion, myoseptum, muscle architecture, teleost, trunk muscle.

Introduction

Active movement by animals depends on deformations in soft tissues, in particular muscles. Muscle architecture is constrained by the physical properties of matter, by functional demands and by phylogenetic limitations, leading to preferred (attractor) regions in morphospace. The importance of physical constraints for the design of a muscle–tendon system will be illustrated in this paper by an analysis of the architecture of the trunk muscles in fish. The trunk muscles in fish and fish-like chordates (in particular cyclostomes and cephalochordates) are arranged in a longitudinal series of myomeres of complex shape (Fig. 1A). The myomeres are separated by collagenous sheets, called myosepta, with a complex fibre arrangement. The lack of insight into the architecture of the myomeres is a long-standing problem in functional morphology.

The trunk muscles have attracted the interest of many morphologists (e.g. Greene and Greene, 1913; Shann, 1914; Kishinouye, 1923; Nishi, 1938). Nursall (1956) provided a comparative overview of myomere shape in cephalochordates, agnathans, selachians and bony fish. In selachians and bony fish (the focus of this report), the myomeres represent a series of nested 'cone-like' structures. More recently, Westneat et al. (1993) described the morphology of the myomeres in scombroid fishes. Gemballa (1995) gave a comparative overview of the myomeres in Actinopterygii.

In most fishes, slow-twitch muscle fibres are located laterally as a longitudinally orientated superficial band (e.g. Boddeke et al., 1959). The deeper fibres are generally of a faster type and are arranged in more complex three-dimensional arrays. Alexander (1969) distinguished two basic patterns for these deeper fibres. One pattern was found in the myomeres of selachians and 'primitive' bony fishes such as eel (*Anguilla* spp.) and trout (*Salmo* spp.). In these fishes, lateral muscle fibre trajectories extend between the tendons of the anterior and posterior cones of the myosepta. Deeper trajectories run from the tendons to the median plane. The selachian pattern was also found to be present in the caudal part of the trunk of other teleosts, which possess anteriorly a helical arrangement of the muscle fibres. By assuming particular deformations of the body during bending, Alexander (1969) concluded that both patterns result in approximately equal strains of the fibres in the white muscle mass within a single myomere.

Gemballa (1995) disputed some of the findings of Alexander (1969). He found no essential differences between the muscle fibre arrangement in anterior myomeres of selachians and those of bony fish. In his opinion, the selachian myomeres and those of the 'primitive' bony fish analysed by Alexander (1969) were all taken from fairly caudal regions of the body, where (except in cephalochordates and agnathans) the 'selachian' pattern is found in all fish taxa.
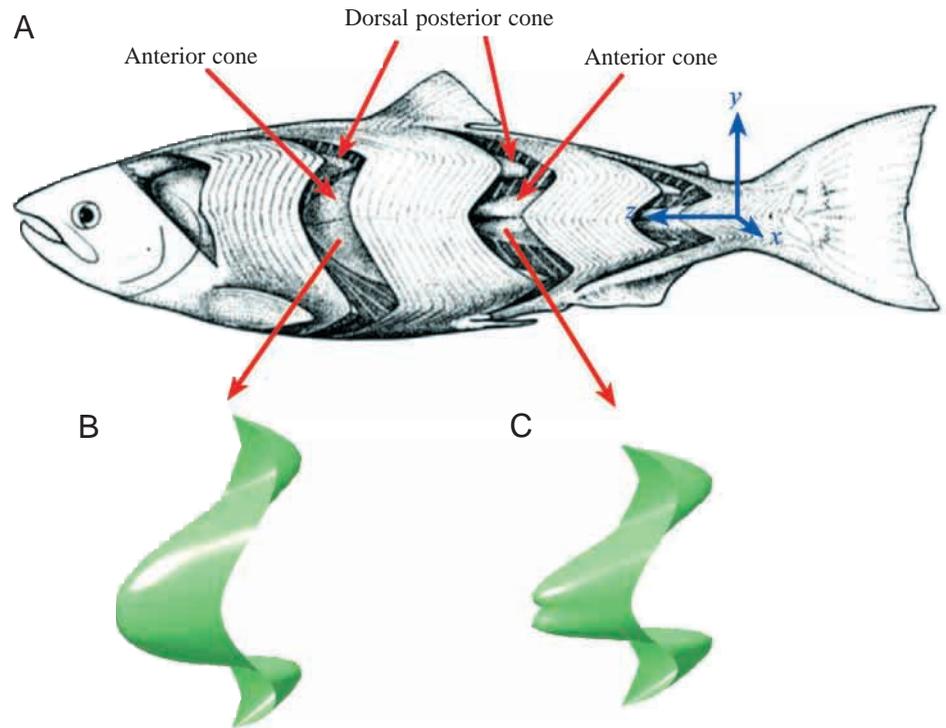
Fig. 1. (A) King salmon, adapted from Greene and Greene (1913). The coordinate system used in the calculations is shown in blue. (B) Simulated shape of a mechanically stable anterior myoseptum (see Fig. 2 for details and Fig. 3 for a stereoscopic view). (C) Simulated shape of a posterior myoseptum (see Fig. 4 for details).

Alexander (1969) calculated average strains for the muscle fibre trajectories, although the deformation of the trunk could result in varying local strains along one trajectory. This suggestion is supported by electromyographic studies that show a delay in muscle activity down the trunk during cyclic swimming (e.g. Van Leeuwen et al., 1990) and intermittent swimming (e.g. Jayne and Lauder, 1994). During burst-and-glide swimming in largemouth bass (*Micropterus salmoides*), muscle fibres of a single myomere are simultaneously active (except for the most dorsal and ventral parts, which are inactive during this swimming mode), whereas activation is progressively delayed in a caudal direction (Jayne and Lauder, 1995).

Relatively few studies have described the collagen fibre arrangement in the myosepta. Westneat et al. (1993) described, from careful dissections, two main collagen fibre orientations in the myosepta of scombroid fishes. One group of fibres is orientated more or less longitudinally, whereas another group has a circular arrangement in the dorsal and ventral main anterior cones. Using polarized light microscopy, Gemballa (1995) observed two main collagen fibre arrangements in the epaxial myosepta in actinopterygians and selachians. One system (the lateral band) runs from the tip of the dorsal anterior cone *via* the lateral part of the myoseptum to the tip of the dorsal posterior cone. The other system (the epineural ligament) runs caudo-laterally within the dorsal part of the dorsal anterior cone. Similar systems are found in the caudal hypaxial muscles.

Most fish species, but not all, have a horizontal septum (for instance, it is absent in *Galeus*, *Latimeria*, *Acipenser* and *Lepisosteus*; see Gemballa, 1995) that divides the trunk muscles into epaxial and hypaxial parts. The horizontal septum contains a cross-ply arrangement of collagen fibres that are believed to play a role in the transmission of forces from the muscle fibres (Westneat et al., 1993; Gemballa, 1995). The collagen fibres are often 'condensed' in conspicuous ligaments.

In his analysis of muscle fibre strain in teleosts, Alexander (1969) did not include the myosepta. Nevertheless, these structures are likely to play a role in transmitting muscle fibre forces. In this paper, I propose that these structures probably serve to diminish the work done on each other by serially arranged muscle fibres with non-uniform activations.

For a given longitudinal strain of the muscle fibres, much higher curvatures occur posteriorly in the trunk of a teleost fish compared with anterior locations (saithe *Pollachius virens* and mackerel *Scomber scombrus*; Videler and Hess, 1984). Only limited variations in strain amplitude occur down the trunk (peak strains tend to increase slightly in a caudal direction). For instance, Katz et al. (1999) have shown that the peak longitudinal red muscle fibre strain increases only modestly along the trunk in milkfish (*Chanos chanos*) during cyclical swimming and sprint swimming (above 2.6 fork lengths s^{-1}). For the laterally positioned red muscle fibres, this is mainly achieved by the decreasing distance between the muscle fibres and the axis down the trunk (Van Leeuwen et al., 1990). This argument does not hold for the fast fibres since, both anteriorly and posteriorly, white fibres are present at identical small distances from the median plane. Strain equalization must originate partly from different fibre orientations along the trunk. Different orientations have indeed been observed, but the mechanical consequences are not well understood.

The shape of the myomeres varies along the trunk (Fig. 1A). In teleosts, the anterior cones are relatively large in the anterior region, whereas the posterior cones are fairly small. The

relative size of the anterior cones diminishes gradually down the trunk, whereas the posterior cones increase their relative size. In addition to changes in size, the cones also change shape as a function of location. The anterior cone may have a single apex anteriorly that touches the vertebral column. Posteriorly, the anterior cone is generally bifid, with the apices lying free in the muscle tissue.

Van der Stelt (1968) attempted to derive the orientation of the myosepta and muscle fibres from the functional demand of equal work output by fibres from different locations. In a planar model study, he found two distinct solutions for this problem that corresponded well with the architecture of particular horizontal sections through the trunk muscles of the lamprey (*Lampetra* sp.) and the smelt (*Osmerus* sp.). However, Van der Stelt (1968) treated the myosepta as inextensible, considered only infinitesimal deformations and neglected the physical demand of mechanical stability as outlined by Van Leeuwen and Spoor (1992, 1993) for skeletal muscles. Nevertheless, he was the first, to my knowledge, to attempt to predict quantitatively (and fully analytically) some architectural aspects of the trunk muscles. From an architectural model, Van Leeuwen (1994) suggested that the large differences in myomere design found in lampreys, selachians and bony fish lead to different gearing ratios and that lampreys undergo larger body curvatures than teleosts for similar amplitudes of muscle fibre strain, whereas teleosts produce the largest bending moments.

In spite of an extensive literature on muscle function in fish swimming, the architecture of the trunk muscles is still poorly understood. In the present paper, I attempt to generate muscle architectures from physical principles and functional demands. Mechanically stable solutions for three-dimensional myomere architectures will be proposed by considering differences in the local muscle fibre tension at opposite sides of the myoseptum. The term 'stability' has different meanings in different disciplines such as orthopaedics, control theory and various branches of mechanics. The starting point here is that the laws of classical mechanics are applicable and that muscles should be designed to generate and transmit forces effectively (excluding some exceptional cases). For instance, one portion of a muscle should not do work on another portion by stretching it forcefully; otherwise, external work and efficiency would be reduced. The resting configuration of a skeletal muscle is therefore generally rather similar to its stress situation. The shapes cannot be the same in both situations because force-producing muscle fibres stretch tendinous sheets and tendons. A muscle that first deforms significantly and dissipates energy internally before it can produce a useful mechanical interaction with its direct environment (this also includes energy absorption, e.g. during landing after a jump) would be classified as mechanically unstable.

The present approach uses similar starting points to those used by Van Leeuwen and Spoor (1992, 1993) to generate the shape of skeletal muscles. They developed a planar model, whereas a three-dimensional approach is proposed here. By prescribing muscle fibre orientations that correspond approximately to anterior and posterior locations, different myomere shapes will be generated that will be qualitatively compared with actual shapes. Some attention will also be paid to the mechanical role of the skin and intramuscular bones and to the mechanical interaction between myomeres and medial fins. In addition, I present new quantitative data on the muscle fibre length distribution in a myomere of a mackerel.

Materials and methods

The model developed in this paper generates architectural predictions such as myomere shape. Most predictions will be tested against data from the literature. For one prediction, i.e. that a helical arrangement of the muscle fibres must lead to considerable variations in muscle fibre length within a myomere, no appropriate data set was found. To fill this gap, I studied the fibre length distribution in the sixteenth myotome of one specimen of mackerel (*Scomber scombrus*, fork length 394 mm), which was smoked and steamed to allow easy dissection of thin layers of muscle fibre bundles. The three-dimensional positions of the anterior and posterior myoseptal attachments of several hundred muscle fibre bundles were measured using a video system in combination with three orthogonal magnetic rulers (effective spatial accuracy of approximately 0.1 mm; fibre length varied from approximately 2 mm to 17 mm). The length of the individual fibres was estimated as the linear distance between their attachment points. This procedure tends to underestimate the real lengths slightly (because the fibres are often slightly curved), especially for the longest fibres. No corrections were made for possible effects of the 'preparation' of the fish. More accurate measurements were impossible in the time available. Length differences among the fibres were, however, much larger than could be attributed to measurement errors (approximately 0.25 mm).

The model

Starting points: why are myosepta needed?

First, I discuss the model used to generate myomere shapes. The central idea behind the present approach is the application of the concept of mechanical stability, as outlined in the Introduction. I have not attempted to derive both the muscle fibre orientations and the myomere shape. For this purpose, a dynamic model of multiple segments would be required, which is beyond the scope of the present study. Instead, muscle fibre orientations similar to those found in real fish were prescribed, and the myotome shape was calculated from the mechanical stability demands of the myoseptum.

Myosepta are required for (at least) the following reasons. Adjacent muscle fibres on opposite sides of a myoseptum can transfer different tensile stresses because of differences in activation, orientation, strain, strain rate and cross-sectional area. Without a myoseptum, the force difference could lead to internal losses of power (a muscle fibre that is forcibly stretched by other fibres absorbs energy). The myoseptum

could ensure mechanical equilibrium if it effectively counteracts, at each position, the unbalance in muscle fibre force. In this way, the myoseptum functions as a sheet that transmits (1) forces between different muscle locations (this is unlikely to solve the instability problem on its own) and (2) forces to the medial plane (occasionally *via* tendons that originate from the cone apices in some species), skin and horizontal septum. The forces mentioned under 2 could contribute in a useful way to lateral bending, thereby enhancing the efficacy of the muscular system. The non-uniformly distributed elastic properties of the myoseptum should be included in a mechanical analysis of this problem.

Thus, the series of (mechanically stable) myosepta provides the freedom to delay the muscle fibre excitation along the trunk of the fish, as observed for cyclic swimming by various authors (e.g. Williams et al., 1989; Van Leeuwen et al., 1990), without serious internal energy losses inside the muscle tissue. My design hypotheses also agree with the observation that, during burst-and-glide swimming in largemouth bass muscle fibres of a single myotome in the region of the main anterior cone are active simultaneously, whereas activation is progressively delayed in a caudal direction (Jayne and Lauder, 1995).

Simplifying assumptions

The five most important assumptions made in the model were as follows.

(1) The intramuscular pressure was taken to be identical on both sides of the tendinous sheet. This is allowed only if the tensile stresses in the muscle fibres are very high compared with the pressure. The difference in skeletal muscles is generally five- to tenfold (Van Leeuwen and Spoor, 1992).

(2) Anterior fibres were assumed to exert slightly higher tensile stresses than their neighbouring posterior fibres in the region around the horizontal septum, whereas the reverse situation was assumed for the dorsal and ventral regions. This leads to a relatively simple loading regime that produces fairly realistic shapes (see Results and Discussion). At slow and medium swimming speeds, muscle fibres in the region of the anterior cones tend to be predominantly active (Jayne and Lauder, 1995), while the onset of activation is delayed in a posterior direction. Consequently, the anteriorly attached muscle fibres exert higher forces on the anterior cone of a myoseptum than do the posteriorly attached fibres (in addition, the anterior cones decrease in size along the trunk). Therefore, forces must be transmitted posteriorly (towards the dorsal and ventral cones in teleosts) along the myoseptum, and a reversal of the direction of the external load on the myoseptum is likely to occur at some point (as indicated by tendons that are attached to the posterior cones in some species). Note also that, compared with the anterior cones, the relative size of the posterior cones increases down the trunk. Future electromyographic studies are required to improve our understanding of the role of the muscle fibres in the region of the dorsal and ventral posterior cones in teleosts.

(3) The collagen fibres in the myoseptum were assumed to function as linear tensile springs that cannot resist compressive forces. This assumption was made only to simplify the calculations of the initial version of the model. In forthcoming work, this assumption will be relaxed to include spring non-linearities and simulation of bony elements.

(4) To simplify geometric considerations, the myomeres were assumed to occupy the entire space between the skin and the median plane. No space was reserved for the vertebral column, bony elements, nerves, etc.

(5) External fluid-dynamic forces were neglected. The intramuscular pressure will be influenced by external fluid pressures. Outward bulging of the skin between adjacent myosepta can be seen in swimming sharks (J. L. Van Leeuwen, personal observation), indicating that the local superficial intramuscular pressure exceeds the external fluid pressure on the skin.

Calculations of myomere shape

A Cartesian coordinate system was used, with the *x*-axis pointing in the transverse direction of the fish, the *y*-axis in the dorsoventral direction and the *z*-axis in the longitudinal direction (Fig. 1A). The *y,z* plane (*x*=0) represents the median plane. The *x,z* plane (*y*=0) will be denoted as the mid-frontal plane, the *x,y* plane as the transverse plane. Longitudinal collagen fibre strains (ε_{CF}) were calculated as:

$$\varepsilon_{CF} = (l_{CF} - l_{CF0})/l_{CF0}, \tag{1}$$

where l_{CF} is fibre length and l_{CF0} is the reference length. Calculations were performed for one myoseptum only (on one side of the body). The following five main steps were taken in the calculations.

(1) The shape of the model myoseptum ('the sheet') was defined by the positions of an array of knot points. Initially, these points were assumed to lie in one transverse plane (the *x,y* plane, see Fig. 2A). The knots were interconnected by linear springs with a prescribed stiffness. The net of interconnected springs represented the collagen fibres in the myoseptum. The knots and springs at the lateral surface were considered to lie in the skin. The springs in the skin were given a much higher stiffness (i.e. approximately two orders of magnitude higher) than the internal springs. This corresponds to the much greater thickness of the skin compared with that of the myosepta. Local body dimensions were prescribed, such as the lateral width-to-height ratio. All parameters were defined in dimensionless form. All length dimensions were normalized with respect to the local initial half-width of the fish. At each knot, a small point mass was assigned for calculation purposes (see step 4). The initial outer shape (the skin boundary) was defined to be elliptical, and the initial boundary with the median plane was a straight line.

(2) A spatial vector field was prescribed which defined the direction of the muscle fibres at each knot position. This field was independent of time. For each knot, the muscle fibre direction was assumed to be identical for the connecting anterior and posterior muscle fibres. A helical arrangement was prescribed for the fast muscle fibres, whereas a longitudinal orientation was chosen for a group of slow muscle fibres on
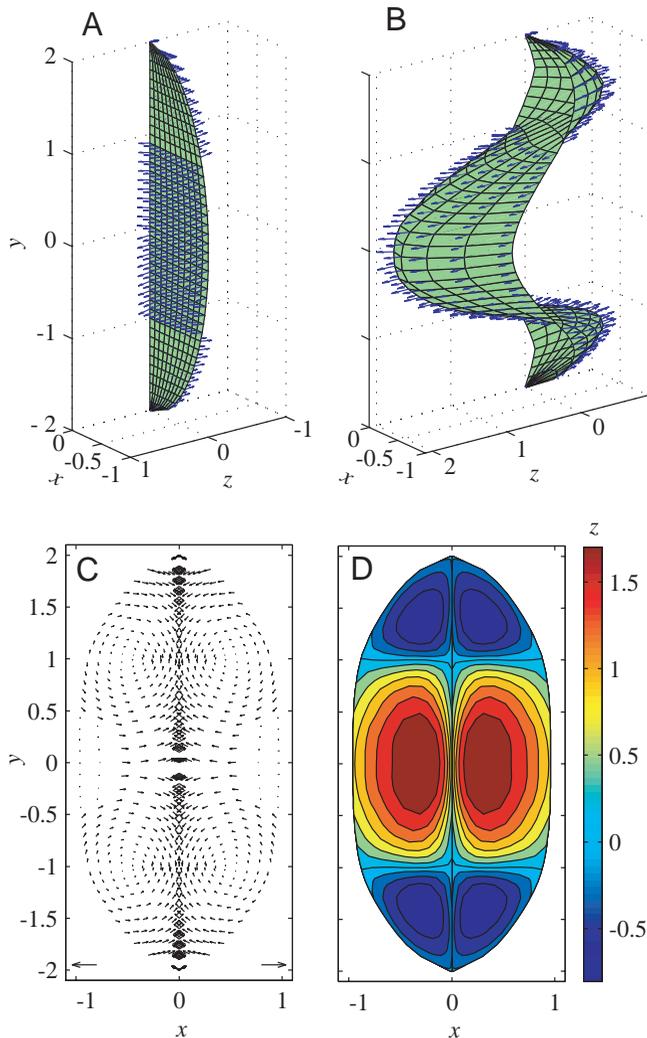
Fig. 2. Results of a simulation of the architecture of an anterior myomere. The presence of the abdominal cavity and vertebral column were ignored. (A) Start configuration of a myoseptal sheet with local force directions indicated by arrows. (B) Configuration of the deformed net at mechanical equilibrium. (C) Projection of unit vectors of force direction on the transverse plane. The arrows in the lower left and right corners show the lengths of unit vectors that are parallel to the x,y plane. Note the lateral regions of longitudinally orientated fibres. (D) Contour plot of the caudal–rostral position of the sheet. This picture may be loosely compared with a cross section of a fish. Values for the right-hand side only were calculated. The left-hand side is a mirror image of the right-hand side. Further explanation in the main text.

horizontal septum that counteracted the local longitudinal (z) components of the muscle forces (their contribution could be varied to allow the effects of horizontal septum forces on myomere shape to be assessed). The external knots (skin knots) undergo a similar force regime, but a pressure force was included here to keep muscle volume almost constant. The intramuscular pressure (p_M) was calculated as:

$$p_M = c_p(A_{TP} - A_{TP0})/A_{TP0}, \qquad (2)$$

where A_{TP} is the projected surface area enclosed by the skin knots in the transverse plane and c_p is a stiffness constant. A_{TP0} is A_{TP} in the initial configuration. c_p was chosen such that A_{TP} differed by less than 0.1 % from A_{TP0}. The pressure forces on the skin ensure that, globally, the volume remains almost constant. Locally, the volume was allowed to change to achieve considerable initial sheet deformations (otherwise realistic shapes could not be approached). Once these had been established (end of step 4, see below), local volume variations were also restricted (as occurs in the fish). This last step results in a variable pressure over the sheet. In addition, forces were prescribed on the skin knots that were proportional to the knot displacement from the initial position in the z direction (to simulate longitudinal force transmission in the skin, in addition to the transmission in the spring direction at this location).

(4) The displacements of the knots under the influence of simulated muscle fibre forces, spring forces in the sheet and pressure forces were calculated by applying Newton's second law of motion for each knot mass. This leads to a coupled system of second-order ordinary differential equations, which were first rewritten in the equivalent first-order ordinary differential equation system. The knot displacements of this initial value problem were solved numerically. A friction term was added to enhance numerical stability. The integration procedure was stopped when all knot speeds and accelerations were close enough to zero. The final knot positions were considered as the mechanical equilibrium situation. The equilibrium positions of the knots are the main interest here, not the individual pathways of the knots. Other solution techniques could have been applied, but the application of Newton's second law to determine the equilibrium provides an excellent basis for a future extension of the model to dynamic situations. The muscle forces were adjusted in each time step because muscle fibre orientation changes with knot position (see step 2) and local cross-sectional area depends on fibre orientation and the relative positions of the nearest neighbouring knot points (recall the proportionality between the magnitude of the local net muscle force on the sheet and the cross-sectional area of the local muscle fibres). All knots were considered as movable except the initially extreme dorsal and ventral knots in the median plane. Simulations were also made by fixing the position of all knots that were initially in the median plane. Knots were not allowed to penetrate the median plane. Typically, 200 iterations were required.

(5) The end condition of step 4 results in considerable variations among the strains in the springs of the sheet. Such a configuration (with strain amplitudes in the mechanical

the mid-lateral side (see, for example, Fig. 2C). During the simulation (see step 4), the knots were displaced and local fibre directions were adjusted according to the vector field described above. The net muscle fibre forces on the knots were directed along the muscle fibres. The magnitudes of these forces were proportional to the local cross-sectional area.

(3) The forces on internal knots result from the tensile forces of the attached muscle fibres and collagen springs. In addition, boundary forces could be described at the positions of the
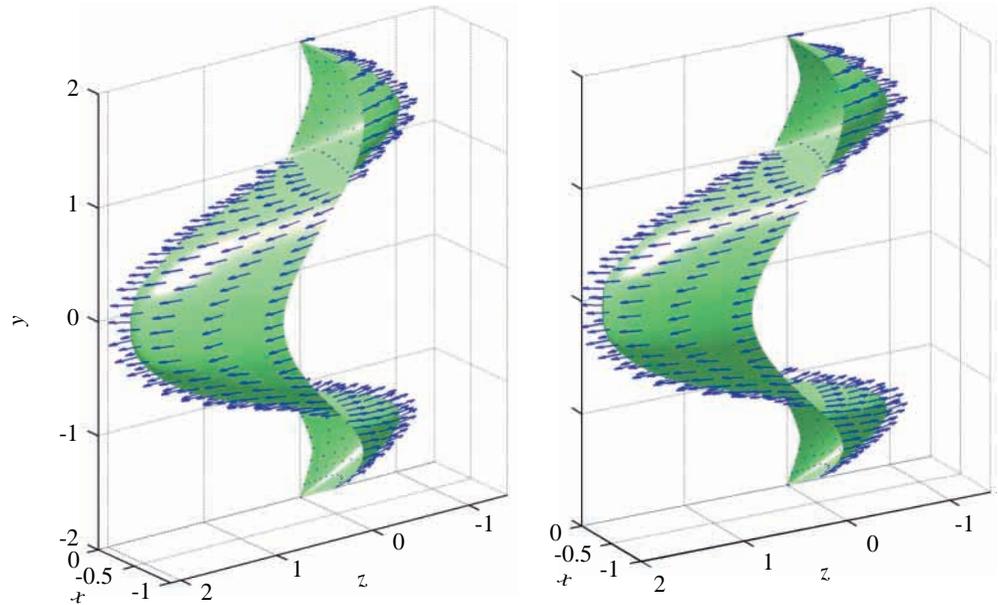
Fig. 3. Stereograph of the simulated myoseptum of Fig. 2. Further explanation in the main text.

failure range for collagen fibres) could not occur in the biological system. The equilibrium configuration obtained using step 4 was therefore used as the starting configuration for a subsequent simulation step. First, all spring constants were given a value proportional to their strain (and, therefore, because of the spring linearity chosen, their tensile force) in the above equilibrium situation if $\varepsilon_{CF}>0$; otherwise, a value of zero was assigned. Second, all strains in the sheet springs were reset to zero (i.e. $\varepsilon_{CF}=0$), so that only muscle fibre forces and pressure forces were present in the new start configuration. As for step 4, knot displacements were calculated until a new mechanical equilibrium was reached. Step 5 resulted in a much more limited strain variation in the springs, with typical strain values of 0.05. A typical number of iterations of step 5 was 100.

The model was implemented in Matlab 5.3 (The MathWorks Inc.).

Results and discussion

In this section, I shall discuss some predicted myotome shapes, which were generated by different initial vector fields for the muscle fibres.

Predicted shape and collagen fibre trajectories for 'teleost-like' myomeres

Fig. 2A shows the starting configuration of the sheet for a simulation of the geometry of an anterior myoseptum. The abdominal cavity was not included for reasons of simplicity. Fibre trajectories can be discerned that run from medial to lateral and from bottom to top. Each knot is connected to four springs (except for outer boundary knots). The initial height of the sheet was $4w_H$, where w_H is the initial half-width. Prescribed directions of muscle fibre forces are shown by small blue arrows. Posteriorly directed forces from the horizontal septum

(other than muscle fibre forces at this location) were not introduced in this simulation. Indeed, the posterior oblique tendons are weakly developed and make a small angle with the transverse plane in the anterior body region (e.g. in *Scomberomorus cavalla*; see Fig. 5A of Westneat et al., 1993). More posteriorly, the posterior oblique tendons play a major role in transmitting forces that make an angle with the myoseptal surface. In anterior myosepta of bony fish, epipleural ribs are generally present at the level of the horizontal septum. Fig. 2B shows the final equilibrium configuration of the deformed net, with a single dominant main anterior cone, a small epaxial posterior cone and a small hypaxial posterior cone and with the direction of the muscle forces again indicated by arrows. The lengths of the springs are roughly proportional to the locally transmitted force. The same simulated shape is shown in Fig. 1B, as a comparison with an anterior myotome of a salmon, and in Fig. 3 as a stereograph. Fig. 2C shows the projection of the force directions of the muscle fibres (located at the knots) on the transverse plane after deformation. A helical architecture was prescribed in both the epaxial and hypaxial muscle parts. The centres of the helices were located at $(0.51w_H, w_H, 0)$ and $(0.51w_H, -w_H, 0)$, respectively. To account for the slow-twitch fibres, a region at the mid-lateral side was defined where the muscle fibres were aligned longitudinally. Between the helix centres of the dorsal and ventral musculature, the muscle fibres had a forwardly directed force. Dorsal and ventral to these centres, the muscle forces had a posteriorly directed component.

Fig. 2D shows a contour plot of the caudo-rostral position of the sheet. This corresponds roughly to the familiar nested curves of collagen tissue that can be observed in a fish steak. In the fish steak, however, the collagen 'contours' are contributed by a series of similarly shaped myosepta nested one inside the other along the length of the fish. The contour plot shows clearly that the apices of the left and right anterior
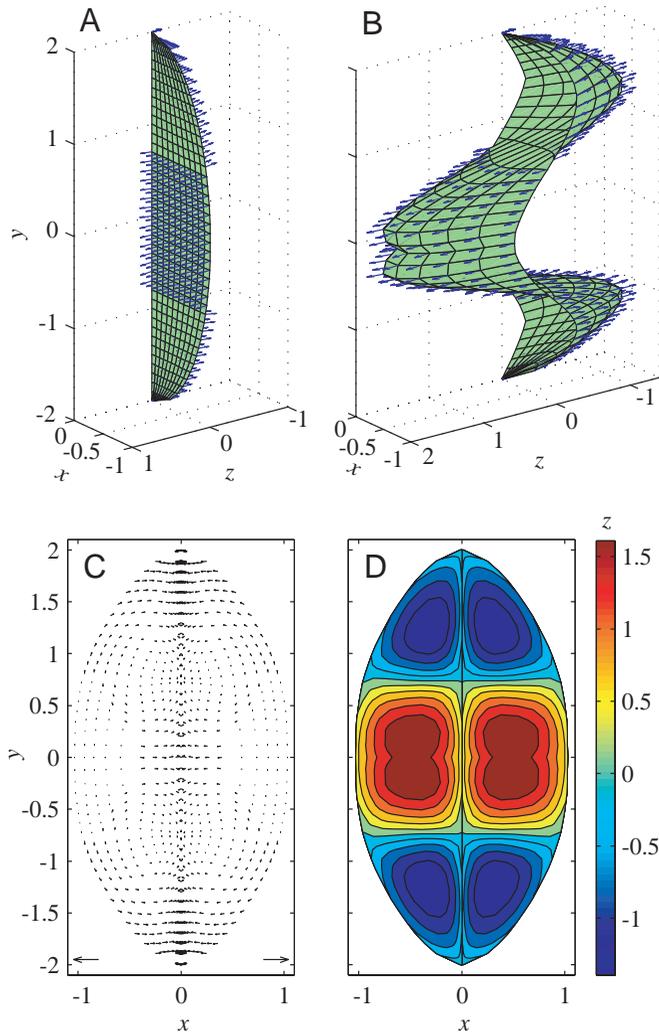
pitch. The curvature of lateral bending is greater posteriorly than anteriorly. Compared with the anterior architecture, the chosen posterior muscle fibre arrangement would reduce the muscle fibre strain for a given curvature of the axis. This leads to a fairly similar strain amplitude along the trunk. At the level of the horizontal septum, posteriorly directed forces at the knots (−0.7 of the local muscle fibre forces) were introduced to simulate the influence of this sheet. Fig. 4B,D shows that the main anterior cone is now bifid and more elongated. The bifid character is caused partly by the altered muscle fibre arrangement and partly by the horizontal sheet forces. The relative size of the anterior cone is smaller than that of Fig. 2, whereas relatively larger posterior cones are present. The apices of the anterior cones are now located at a relatively greater distance from the median plane. These anterior and posterior characteristics correspond to differences down the trunk that can be observed in a real fish. The shape of the simulated myoseptum is also shown in Fig. 1C and allows a qualitative comparison with the shape of a myomere from the anal region in the salmon. The simulations of Figs 2 and 4 show that differences in muscle fibre arrangement have a large effect on the shape of the myomere.

Design and optimal length of the myoseptum

The change in shape from the anterior myoseptum design to the design of the myoseptum of the anal region can be interpreted as an intermediate transformational step towards a tendon. Indeed, in the extreme posterior region, the myosepta generally have a very tendon-like architecture, and in many species 'real' tendons are present (notably, for example, in scombroid fish).

What is the optimal length of a myoseptum from a functional point of view? A relatively short, flat myoseptum must have relatively thick collagen fibre bundles to resist (i.e. deflect not more than a 'functional' amplitude) a particular load. A longer myoseptum can be made thinner, but it overlaps with more vertebral segments. If a myoseptum were too thin, it would overlap with an unpractical number of vertebral segments (from a control point of view). Thus, a balance can be expected between the material invested in the myosepta and demands for adequate movement control by the neuromuscular system. In the posterior region of the fish, the longitudinal force gradient in the muscle fibres is expected to increase. The geometrical consequences are observed in the design as a shortening of the segmental distance and the presence of more-elongate myosepta.

The shape of the myoseptum and the location of median fins

The contour plots of Figs 2, 4 and 5 demonstrate that, in the extreme dorsal and ventral regions, the contours slope towards the sagittal plane, either in a ventral direction or in a dorsal direction. This arrangement is expected to facilitate a more-or-less independent mechanical functioning of the myomeres and the dorsal and ventral median fins.

Effects of skin stiffness on external shape

Fig. 5 shows the effect of skin stiffness on external shape.

Fig. 4. Results of a simulation of the architecture of a posterior myomere. (A) Start configuration of the myoseptal sheet with local force vectors indicated by arrows. (B) Configuration of the deformed net at mechanical equilibrium. (C) Projection of unit vectors of force direction on the transverse plane. The arrows in the lower left and right corners show the lengths of unit vectors that are parallel to the *x,y* plane. (D) Contour plot of the caudal–rostral position of the sheet. This picture may be loosely compared with a cross section of a fish. Values for the right-hand side only were calculated. The left-hand side is a mirror image of the right-hand side. Further explanation in the main text.

cones are fairly close to the median plane. Their position corresponds closely to the lateral border of the vertebral column in a real fish. The boundaries between the anterior cone and the posterior cones correspond to the locations of the centres of the muscle fibre helices. This is in agreement with anatomical observations.

Fig. 4 shows a similar set of panels to those in Fig. 2. The muscle fibre and force directions were, however, chosen to correspond roughly to a myomere from the anal region. The centres of the helices were chosen at $(0.3w_H, w_H, 0)$ and $(0.3w_H, -w_H, 0)$, and the helices were given a slightly higher
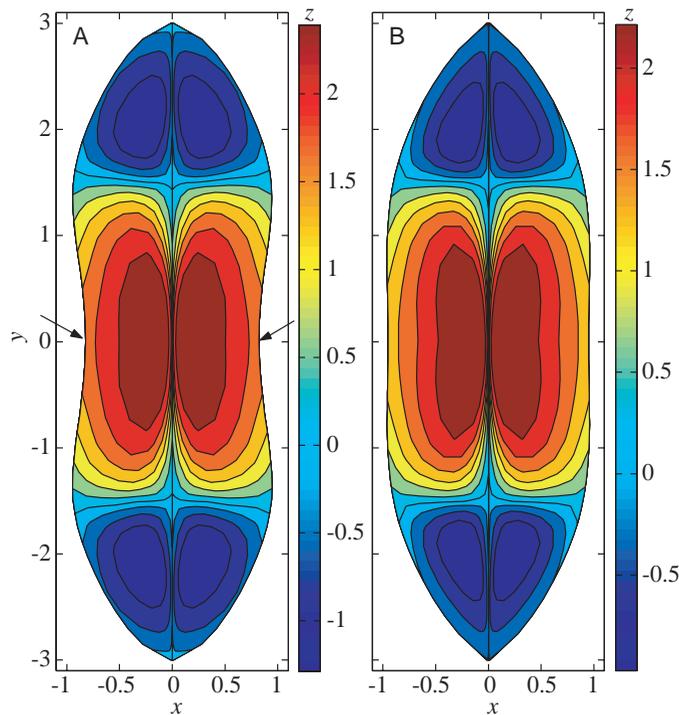
Fig. 5. Results of two simulations showing the effects of skin stiffness. (A) Simulation with similar parameter choice to that in Fig. 1. However, the dimensionless height was increased from 4 to 6, and the skin stiffness was halved. Note the concavities at the level of the horizontal septum (arrows). Too low a skin stiffness leads, in the absence of ribs and intramuscular bones, to large ineffective deformations that would reduce the external work that the muscular system could generate. Mechanical instabilities of this nature can be avoided by (1) bony elements (as present in bony fish), (2) a stiff skin (as present in selachians), and (3) a cross-sectional shape with a relatively low height-to-width ratio. (B) Same simulation as in A, but with skin stiffness increased eightfold. The concavities of A are absent because of the increased skin stiffness.

The initial height-to-width ratio was increased compared with Figs 2–4. It was found that a high ratio increased the 'danger' of mechanical instabilities. In Fig. 5A, the skin stiffness was reduced by 50 % compared with that of Figs 2–4. Muscle tissue moved inwards close to the mid-horizontal plane and outwards in the dorsal and ventral regions. Two concavities at the outer boundaries are the result (arrows in Fig. 5A). This architectural deviation is corrected in Fig. 5B, in which the skin stiffness was increased eightfold compared with Fig. 5A. The greater the height-to-width ratio, the greater the skin stiffness required to avoid the mid-lateral concavities. Alternatively, bony elements in the mid-horizontal plane (found in bony fish) could help to avoid the undesirable deformation. In selachians, intramuscular bones and ribs are absent. The skin must therefore play a dominant role in the mechanical stability of the musculature. The absence of bony elements presumably limits the body shapes that selachians can adopt. It is striking that selachians generally have a fairly low height-to-width ratio
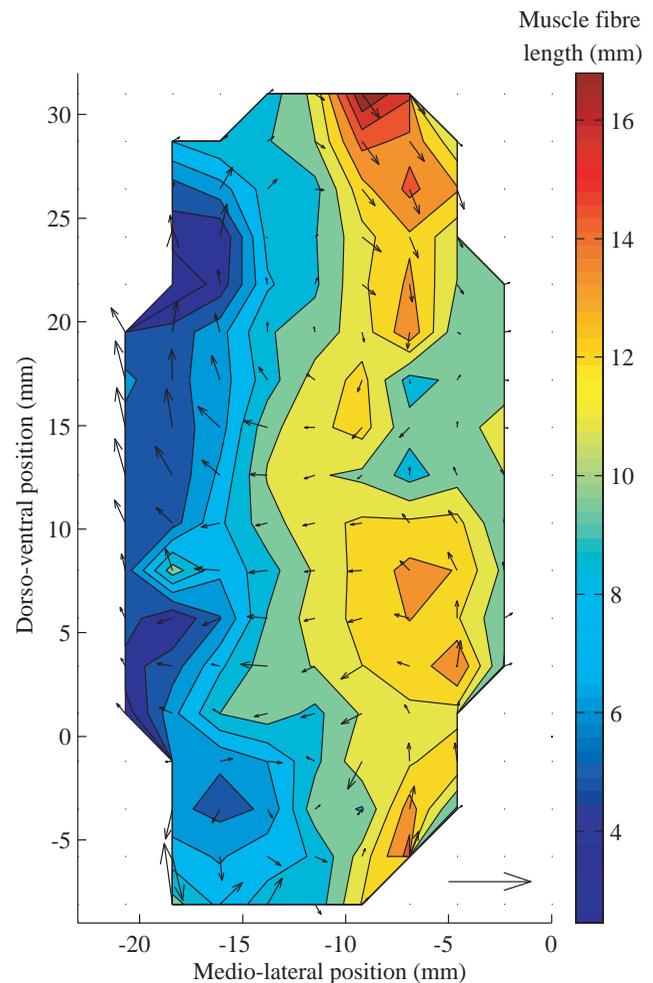

Fig. 6. Contour plot of the distribution of muscle fibre length in the sixteenth myomere of a mackerel. The arrows show the unit orientation vectors of the muscle fibres projected on the transverse plane. The arrow in the lower right corner shows the length of a unit vector that is parallel to the transverse plane. Note the clear helical arrangement of the epaxial musculature and the very considerable variations in muscle fibre length.

along their trunk. The presence of intramuscular bones in bony fish presumably allows a much greater range of possible body forms than would be feasible for selachians.

Variations in muscle fibre length

The combination of the folded shape of the myosepta and the helical arrangement of the muscle must necessarily lead to considerable variations of muscle fibre length within one myomere. This hypothesis is supported by measurements of myomere 16 of a mackerel (Fig. 6). The muscle fibre length was found to vary between 2 and 17 mm. The shortest lengths in the white muscle mass were found close to the median plane, whereas the longest lengths were found latero-dorsally and latero-ventrally. The red muscle fibre systems had intermediate lengths of approximately 10 mm. A clear helical arrangement of the muscle fibres was found in the white epaxial

musculature. Converging fibre directions were found in the hypaxial region, indicating the transition to the caudal muscle fibre arrangement described by Alexander (1969).

General discussion

A quantitative theory is proposed for the prediction of the shapes of the myomeres of fish. By applying the principle of mechanical stability to muscle tissue (as previously proposed by Van Leeuwen and Spoor, 1992, 1993), solutions for myomere shapes were obtained that correspond approximately to the designs found in teleosts. Extensions of the present approach to selachians, cephalochordates and cyclostomes should be possible. The model could be a useful tool in an exploration of the remarkable diversity of myomere shapes in fish.

An interesting finding of the present study is that fairly realistic myoseptal geometries can follow from fairly simple load distributions (see the three regions of Figs 2 and 4). In reality, the mechanical load on the myoseptum will vary with time and with the type of activity. The highest loads are expected to occur during fast-starts and turning manoeuvres. These modes of swimming require almost complete activation of the myomeres. These extreme loading situations, probably dominating geometrical requirements, were selected as the best starting point in this initial study of myomere architecture. At low and intermediate swimming speeds, myomeres are only partially activated, probably mostly in the region of the anterior cones. Additional work is needed to elucidate the internal loading and architectural requirements of the *in vivo* range of functional repertoires.

The shape change occurring in the simulated sheet between the relaxed and the loaded situation, and the resulting force trajectories in the surface, are directly coupled because the distances between the knots determine the strains and forces (their amplitude and direction) in the springs. Interestingly, the simulated sheet, a complex interconnected array of linear springs (each roughly adapted to the individual load after simulation step 5), behaves as a non-linear spring (for instance, caused by changing spring directions during loading) with anisotropic properties that vary over the surface. Clearly, non-linear springs are not required to evoke non-linear behaviour at the macroscopic level of the sheet. Nevertheless, the introduction of non-linear springs will have some consequences for the behaviour of the sheet that could be addressed in future studies. The adaptation of the local sheet properties in a self-organizing process to the strongly non-uniform load distribution and the related geometrical consequences at the macroscopic level go far beyond standard engineering designs. The constructional principles outlined (combining functional demands, mechanical principles and tissue adaptiveness to mechanical loads) are of interest for a better understanding of the phylogenetics and morphogenesis of an important constituent of the vertebrate body plan.

The main force trajectories in the simulated sheets can be compared with observations on collagen fibre trajectories from the literature. The trajectories that run parallel to the horizontal plane in the main anterior cone (Figs 2B, 4B) correspond to the anterior oblique tendons that have been described by various authors (e.g. Westneat et al., 1993; Gemballa, 1995). The trajectories that run more or less longitudinally from the anterior cone to the epaxial and the hypaxial cones correspond to the longitudinal trajectories described by Westneat et al. (1993) and to part of the lateral band of Gemballa (1995). The trajectories that run from the skin surface to the apices of the posterior cones correspond to trajectories shown in a drawing of Gemballa (Fig. 5.5b in Gemballa, 1995). Just dorsal to the horizontal septum, a region with diagonally deformed net elements is present. From a mechanical point of view, these elements could be partly replaced by diagonal trajectories corresponding to the position of the epineural ligament observed by Gemballa. Thus, there is a reasonable correspondence between the main force trajectories of the model and the observed collagen fibre arrangements. This supports the chosen load distribution (partly based on muscle fibre directions) and, therefore, the fidelity of the simulated macroscopic shapes. Currently, I have extended the model to allow not only fibre reinforcement but also the formation of bony elements. My latest simulations predict the positions of intramuscular bones corresponding to their locations in real fish. They also show the stabilizing effects of these bones.

The muscle fibre paths in teleosts show very little convergence. Therefore, there is no need to transmit large forces to the myosepta. The myosepta can therefore be relatively thin. In contrast, selachians have converging muscle fibre paths (Wainwright, 1983) that demand considerable transfer of muscle fibre force to collagen fibres. The selachian myosepta are, therefore, relatively stout and supplied with tendons. Compared with teleosts, the myosepta are also likely to transmit more force to the skin.

The present theory is only a small step towards an understanding of myomere organisation. The architectural analysis should address the shape of the myoseptum based on prescribed muscle fibre arrangements and it should also derive both the myomere shape and the muscle fibre orientations. A necessary further step includes the analysis of the dynamic interaction between the two series of myomeres on the two sides of the body during undulatory movements and the coupling between the internal muscle dynamics and the external mechanics of the water.

References

Alexander, R. McN. (1969). The orientation of muscle fibres in the myomeres of fishes. *J. Mar. Biol. Ass. U.K.* **49**, 263–290.

Boddeke, R., Slijper, E. J. and van der Stelt, A. (1959).

Histological characteristics of the body-musculature of fishes in connection with their mode of life. *Proc. K. Ned. Akad. Wet.* C **62**, 576–588.

Gemballa, S. (1995). Vergleichend-anatomische Untersuchungen am Lokomotionsapparat der Actinopterygii. Phylogenetische Rekonstruction und funktionelle Hypothesen. Dissertation, Eberhard-Karls Universität, Tübingen.

Greene, C. W. and Greene, C. H. (1913). The skeletal musculature of the king salmon. *Bull. U.S. Fish.* **33**, 21–59.

Jayne, B. C. and Lauder, G. V. (1994). How swimming fish use slow and fast muscle fibers: implications for models of vertebrate muscle recruitment. *J. Comp. Physiol.* A **175**, 123–131.

Jayne, B. C. and Lauder, G. V. (1995). Are muscle fibers within fish myotomes activated synchronously? Patterns of recruitment within deep myomeric musculature during swimming in largemouth bass. *J. Exp. Biol.* **198**, 805–815.

Katz, S. L., Shadwick, R. E. and Rapoport, H. S. (1999). Muscle strain histories in swimming milkfish in steady and sprinting gaits. *J. Exp. Biol.* **202**, 529–541.

Kishinouye, K. (1923). Contributions to the comparative study of the so-called scombroid fishes. *L. Coll. Agric. Imp. Univ. Tokyo* **8**, 293–475.

Nishi, S. (1938). Muskelsystem. II. Muskeln des Rumpfes. *Bolks. Handb. Vergl. Anat. Wirbelt.* **5**, 351–446.

Nursall, J. R. (1956). The lateral musculature and the swimming of fish. *Proc. Zool. Soc. Lond.* **126**, 127–143.

Shann, E. W. (1914). On the nature of the lateral muscle in Teleostei. *Proc. Zool. Soc. Lond.* **22**, 319–337.

Van der Stelt, A. (1968). Spiermechanica en myotoombouw bij vissen (in Dutch). Thesis, University of Amsterdam, L. J. Veen's Uitgeversmaatschappij N.V., Amsterdam.

Van Leeuwen, J. L. (1994). Shape prediction of fish myomeres. *J. Physiol., Lond.* **479**, 4P–5P.

Van Leeuwen, J. L., Lankheet, M. J. M., Akster, H. A. and Osse, J. W. M. (1990). Function of red axial muscles of carp (*Cyprinus carpio*): recruitment and normalized power output during swimming in different modes. *J. Zool., Lond.* **220**, 123–145.

Van Leeuwen, J. L. and Spoor, C. W. (1992). Modelling mechanically stable muscle architectures. *Phil. Trans. R. Soc. Lond.* B **336**, 275–292.

Van Leeuwen, J. L. and Spoor, C. W. (1993). Modelling the pressure and force equilibrium in unipennate muscles with in-line tendons. *Phil. Trans. R. Soc. Lond.* B **342**, 321–333.

Videler, J. J. and Hess, F. (1984). Fast continuous swimming of two pelagic predators, saithe (*Pollachius virens*) and mackerel (*Scomber scombrus*): a kinematic analysis. *J. Exp. Biol.* **109**, 209–228.

Wainwright, S. A. (1983). To bend a fish. In *Fish Biomechanics* (ed. P. Webb and D. Weihs), pp. 68–91. New York: Praeger Press.

Westneat, M. W., Hoese, W., Pell, C. A. and Wainwright, S. A. (1993). The horizontal septum – mechanisms of force transfer in locomotion of scombrid fishes (Scombridae, Perciformes). *J. Morph.* **217**, 183–204.

Williams, T. L., Grillner, S., Smolljaninov, V. V., Wallén, P., Kashin, S. and Rossignol, S. (1989). Locomotion in lamprey and trout: the relative timing of activation and movement. *J. Exp. Biol.* **143**, 559–566.

Note added in proof

Fig. 5A shows predicted concavities at the level of the horizontal septum resulting from a combination of a high height-to-width ratio of the cross-section, a low stiffness of the skin and absence of intramuscular bones. This combination of features is present in early larval stages of several fish (I examined larvae of common carp, zebra fish and catfish), which do indeed have the predicted concavities.